

# Strategic Design of Catalytic Lysine-Targeting Reversible Covalent BCR-ABL Inhibitors

David Quach,<sup>[a][b]</sup> Guanghui Tang,<sup>[c]</sup> Jothi Anantharajan,<sup>[b]</sup> Nithya Baburajendran,<sup>[b]</sup> Anders Poulsen,<sup>[b]</sup> John L. K. Wee,<sup>[b]</sup> Priya Retna,<sup>[b]</sup> Rong Li,<sup>[b]</sup> Boping Liu,<sup>[b]</sup> Doris H. Y. Tee,<sup>[b]</sup> Perlyn Z. Kwek,<sup>[b]</sup> Joma K. Joy,<sup>[b]</sup> Wan-Qi Yang,<sup>[d]</sup> Chong-Jing Zhang,<sup>[d]</sup> Klement Foo,<sup>\*,[b]</sup> Thomas H. Keller,<sup>\*</sup> Shao Q. Yao<sup>\*,[a][c]</sup>

- [a] Dr. D. Quach, Prof. Dr. S. Q. Yao  
NUS Graduate School for Integrative Sciences and Engineering, 21 Lower Kent Ridge, University Hall, Tan China Tuan Wing, #04-02, Singapore 119077  
E-mail: [chmyaosq@nus.edu.sg](mailto:chmyaosq@nus.edu.sg)
- [b] Dr. D. Quach, Dr. J. Anantharajan, Dr. N. Baburajendran, Dr. A. Poulsen, J. L. K. Wee, P. Retna, R. Li, B. Liu, D. H. Y. Tee, P. Z. Kwek, Dr. J. K. Joy, Dr. K. Foo, Dr. T. H. Keller  
Experimental Drug Development Centre, 10 Biopolis Road, Chromos, #05-01, Singapore 138670  
E-mail: [thkeller@eddc.a-star.edu.sg](mailto:thkeller@eddc.a-star.edu.sg), [klementfoo@gmail.com](mailto:klementfoo@gmail.com)
- [c] Dr. G. Tang, Prof. Dr. S. Q. Yao  
Department of Chemistry, National University of Singapore, Singapore 117543
- [d] W.-Q. Yang, Dr. C.-J. Zhang  
State Key Laboratory of Bioactive Substances and Functions of Natural Medicines and Beijing Key Laboratory of Active Substances Discovery and Druggability Evaluation, Institute of Materia Medica Peking Union Medical College and Chinese Academy of Medical Sciences, Beijing, China, 100050

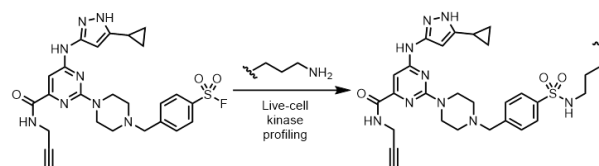
Supporting information for this article is given via a link at the end of the document.

**Abstract:** Targeted covalent inhibitors have re-emerged as validated drugs to overcome acquired resistance in cancer treatment. Herein, by using a carbonyl boronic acid warhead, we report the structure-based design of BCR-ABL inhibitors via reversible covalent targeting of the catalytic lysine with improved single-digit nanomolar potency against both wild-type and mutant ABL kinases, especially ABL<sup>T315I</sup> bearing the gatekeeper residue mutation. We show that, by using techniques including mass spectrometry, time-dependent biochemical assays and X-ray crystallography, the evolutionarily conserved lysine can be targeted selectively. Furthermore, we show that the selectivity depends largely on molecular recognition of the non-covalent pharmacophore in this class of inhibitors, probably due to the moderate reactivity of the warhead. We report the first co-crystal structures of covalent inhibitor-ABL kinase domain complexes, providing insights into the interaction of this warhead with the catalytic lysine. We also employed label-free mass spectrometry to evaluate potential off-targets of our compounds at proteome-wide level in different cancer cell lines.

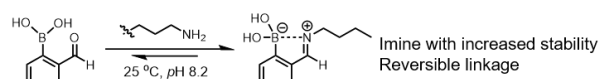
## Introduction

Chronic myeloid leukemia (CML) arises from a genetic abnormality in human chromosome 22, which is unusually short and defective because of the reciprocal translocation of genetic material from chromosome 9.<sup>[1]</sup> Gene expression leads to the formation of a constitutively active BCR-ABL1 kinase, which aberrantly activates multiple signaling pathways that bring about uncontrollable cell growth and differentiation.<sup>[2]</sup> Despite the clinical success of ATP-competitive inhibitors,<sup>[3]</sup> a significant number of patients

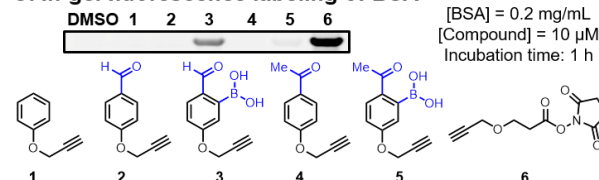
### A. Reported lysine modification by Taunton<sup>[22]</sup>



### B. Iminoboronate mechanism<sup>[30]</sup>



### C. In-gel fluorescence labeling of BSA

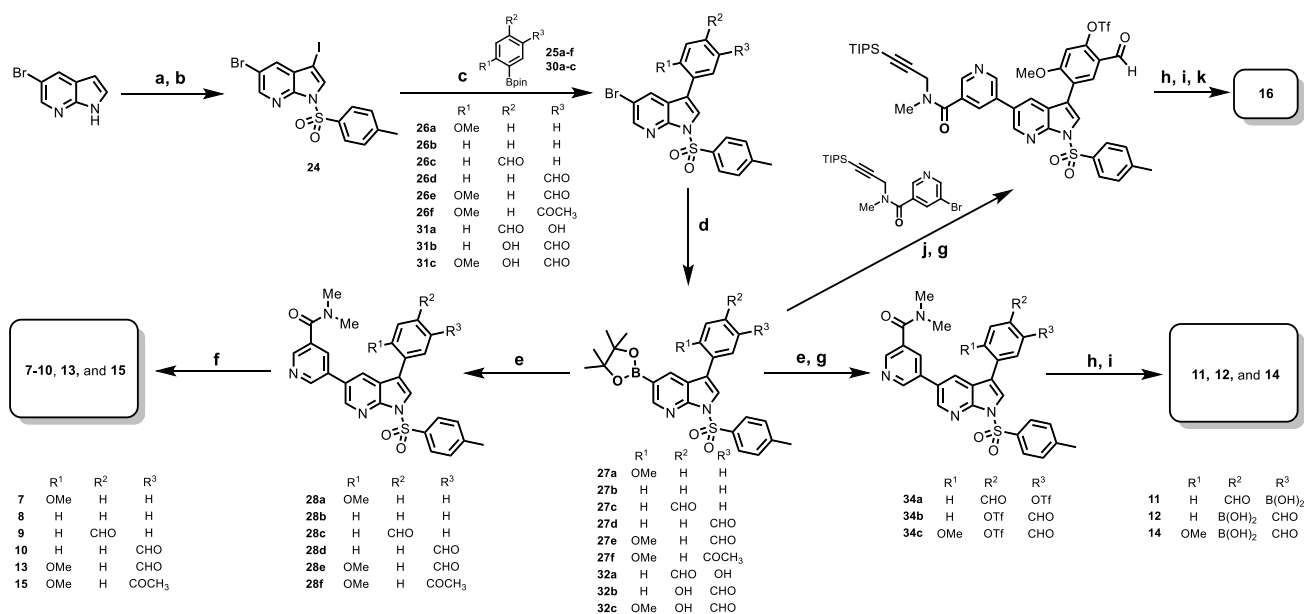


### D. This work



**Figure 1.** (A) A previously reported sulfonyl fluoride probe for covalent lysine labeling of kinases in live cells.<sup>[22]</sup> (B) Lysine modification based on the formation of a stable iminoboronate with 2-formylbenzene boronic acid.<sup>[30]</sup> (C) Model study of various lysine-targeting probes by using bovine serum albumin (BSA). (D) Structure-based design of BCR-ABL inhibitors targeting the catalytic lysine K271, based on a previously reported inhibitor PPY-A (7).<sup>[32]</sup>

have suffered from relapse due to drug resistance, which can arise from point mutations that severely reduce the effect of such inhibitors.<sup>[4,5]</sup> An important mutant in CML is BCR-ABL<sup>T315I</sup> which can only be inhibited by ponatinib (Iclusig).<sup>[6]</sup> Targeted covalent



**Scheme 1.** Synthesis of key inhibitors used in this work. (a) NIS, acetone, rt, 1 h, 98%; (b) TsCl, NaH, THF, 0 °C, 3 h, 96%; (c) Pd(dppf)Cl<sub>2</sub>, K<sub>2</sub>CO<sub>3</sub>, 1,4-dioxane/H<sub>2</sub>O (9:1), 70 °C, 7 h, 60-80%; (d) B<sub>2</sub>pin<sub>2</sub>, Pd(dppf)Cl<sub>2</sub>, KOAc, 1,4-dioxane, 100 °C, 7 h, 70-90%; (e) 5-bromo-*N,N*-dimethylnicotinamide, Pd(dppf)Cl<sub>2</sub>, K<sub>2</sub>CO<sub>3</sub>, 1,4-dioxane/H<sub>2</sub>O (9:1), 95 °C, 7 h, 70-80%; (f) LiOH, MeOH/dioxane/H<sub>2</sub>O (2:2:1), rt, 1 h, up to 90%; (g) CF<sub>3</sub>SO<sub>2</sub>Cl, K<sub>2</sub>CO<sub>3</sub>, DMF, rt, 2-4 h, 80-90%; (h) B<sub>2</sub>pin<sub>2</sub>, Pd(dppf)Cl<sub>2</sub>, KOAc, 1,4-dioxane, 100 °C, 7 h; (i) Cs<sub>2</sub>CO<sub>3</sub>, THF/MeOH (2:1), 40-50 °C, 1 h, 10-20% (2-step yields from (h) and (i)); (j) 5-bromo-*N*-methyl-*N*-(3-(triisopropylsilyl)prop-2-yn-1-yl)nicotinamide, Pd(dppf)Cl<sub>2</sub>, K<sub>2</sub>CO<sub>3</sub>, 1,4-dioxane/H<sub>2</sub>O (9:1), 95 °C, 7 h, 80-90%; (k) TBAF, THF/H<sub>2</sub>O, rt, 2.5% (3-step yield from (h), (i) and (k)).

inhibitors offer advantages such as greater potency and prolonged duration of action over non-covalent inhibitors, and they have reemerged in recent years as demonstrated by the clinical success of, for example, osimertinib.<sup>[7-11]</sup> The standard strategy to design irreversible kinase inhibitors uses Michael acceptors to target poorly conserved cysteine residues near the active site of kinases.<sup>[12]</sup> This was thought to provide a measure of selectivity; however, Cravatt and coworkers have demonstrated that even carefully designed cysteine-targeting covalent inhibitors have off-target effects.<sup>[13]</sup> Furthermore, resistance mechanisms including cysteine point mutations (EGFR<sup>C797S</sup> and BTK<sup>C481S</sup>) often render cysteine-targeting covalent drugs ineffective.<sup>[11]</sup> To our knowledge, no covalent drugs against any of the known BCR-ABL mutants have been reported up to date due to a lack of targetable cysteine residues.<sup>[14]</sup>

Since the catalytic lysine residue is essential for the enzymatic activity of all protein kinases and therefore, considered less prone to mutation,<sup>[15,16]</sup> we have been interested to study this evolutionarily conserved residue in the ATP pocket with the aim to produce covalent kinase inhibitors as an alternative strategy in drug design. Many non-selective lysine-modifying probes, including the use of sulfonyl fluorides and activated esters, have been reported.<sup>[17-23]</sup> Taunton and coworkers were the first who reported sulfonyl fluoride probes for lysine-targeting in kinases (Figure 1A).<sup>[22]</sup> Campos et al later identified lysine-targeting kinase inhibitors that used an activated ester.<sup>[23]</sup> Since cellular toxicity is a major concern for both tool compounds and

drug candidates, many research groups aspire to tune the reactivity of covalent warheads.<sup>[24-28]</sup> For example, Taunton and co-workers used electron-deficient Michael acceptors for the design of cysteine-targeting reversible covalent kinase inhibitors.<sup>[29]</sup> Iminoboronates have recently been shown to reversibly but covalently modify amino groups in proteins;<sup>[30]</sup> however, this chemistry, to the best of our knowledge, has not been used to develop covalent kinase inhibitors (Figure 1B).<sup>[31]</sup> Our aim was therefore to design reversible, covalent inhibitors targeting the catalytic lysine residue in kinases as a general approach to combat drug resistance. We report herein the first successful examples of lysine-targeting reversible covalent kinase inhibitors based on iminoboronate chemistry (Figure 1C/D); our results showed that such compounds possessed potent and long-lasting inhibition against BCR-ABL wild type and mutants.

## Results and Discussion

At the outset, a mechanistic study was carried out to compare the relative reactivity of model probes **3** and **5** with an NHS probe (**6**) and other controls by using BSA as reference (Figure 1C); removal of either carbonyl or boronic acid (or both; e.g. **1**, **2** and **4**) caused complete abolishment in fluorescent labeling of BSA in **3** and **5**. Between **3** and **5**, the former consistently labeled BSA more strongly, indicating the aldehyde was more reactive than the ketone. As expected, both **3** and **5** produced much weaker fluorescence labeling of BSA compared to **6**, suggesting iminoboronates have attenuated lysine reactivity compared to the highly

reactive NHS-based irreversible lysine modifier.<sup>[18]</sup> We next designed suitable iminoboronate-containing BCR-ABL kinase inhibitors (Figure 1D). Molecular modeling studies were first carried out by incorporating a carbonyl boronic acid warhead into a previously reported ABL1 inhibitor PPY-A (**7**) (PDB ID: 2QOH; Figure S1);<sup>[32]</sup> results showed that introducing the required functionality would not disrupt the binding to the protein, and with the distance between the proposed carbonyl boronic acid and the highly flexible catalytic lysine K271 being ~3.5 Å, formation of an iminoboronate in the kinase/inhibitor complex was indeed possible.

A library of analogs was synthesized in order to establish structure-activity relationship (Figures 1D and S2, Scheme 1). The synthesis of a common intermediate **24** was done in two steps via iodination and tosylation of 5-bromoazaindole. **7-10** were obtained in four steps via Suzuki-Miyaura coupling reactions involving **24** to generate **26a-d**, which underwent Miyaura borylation that led to **27a-d**. The Suzuki-Miyaura cross coupling reaction was performed at a lower temperature of 60 °C in order to chemoselectively differentiate Br and I. **27a-d** then underwent a second

Suzuki-Miyaura coupling reaction with 5-bromo-*N,N*-dimethylnicotinamide followed by subsequent removal of tosyl group with LiOH, leading to the formation of the desired inhibitors. The synthesis of carbonyl boronic acid inhibitors **11** and **12** occurred via a different route in which an additional step involving the conversion of OH to OTf, led to intermediates **34a** and **34b**; CF<sub>3</sub>SO<sub>2</sub>Cl and K<sub>2</sub>CO<sub>3</sub> were shown to be the optimal choice. Other electrophiles such as PhNTf<sub>2</sub> and (CF<sub>3</sub>SO<sub>2</sub>)<sub>2</sub>O in the presence of bases such as triethylamine, NaH and pyridine did not work well, however, despite heating. **34a** and **34b** underwent borylation and subsequent deprotection of the tosyl group by using Cs<sub>2</sub>CO<sub>3</sub> was carried out to generate covalent inhibitors **11** and **12** (Supporting Information).

By using a mobility shift assay based on Caliper's microfluidics capillary electrophoresis, the IC<sub>50</sub> value of PPY-A (**7**) against wildtype ABL was determined to be 2 nM (Figure S2). Removal of the *o*-methoxy group reduced the potency by 20 folds (compound **8**). Introduction of *m*-aldehyde (compound **10**), however, improved the IC<sub>50</sub> to 8 nM. Shifting the aldehyde functional group to the *para* position was not tolerated

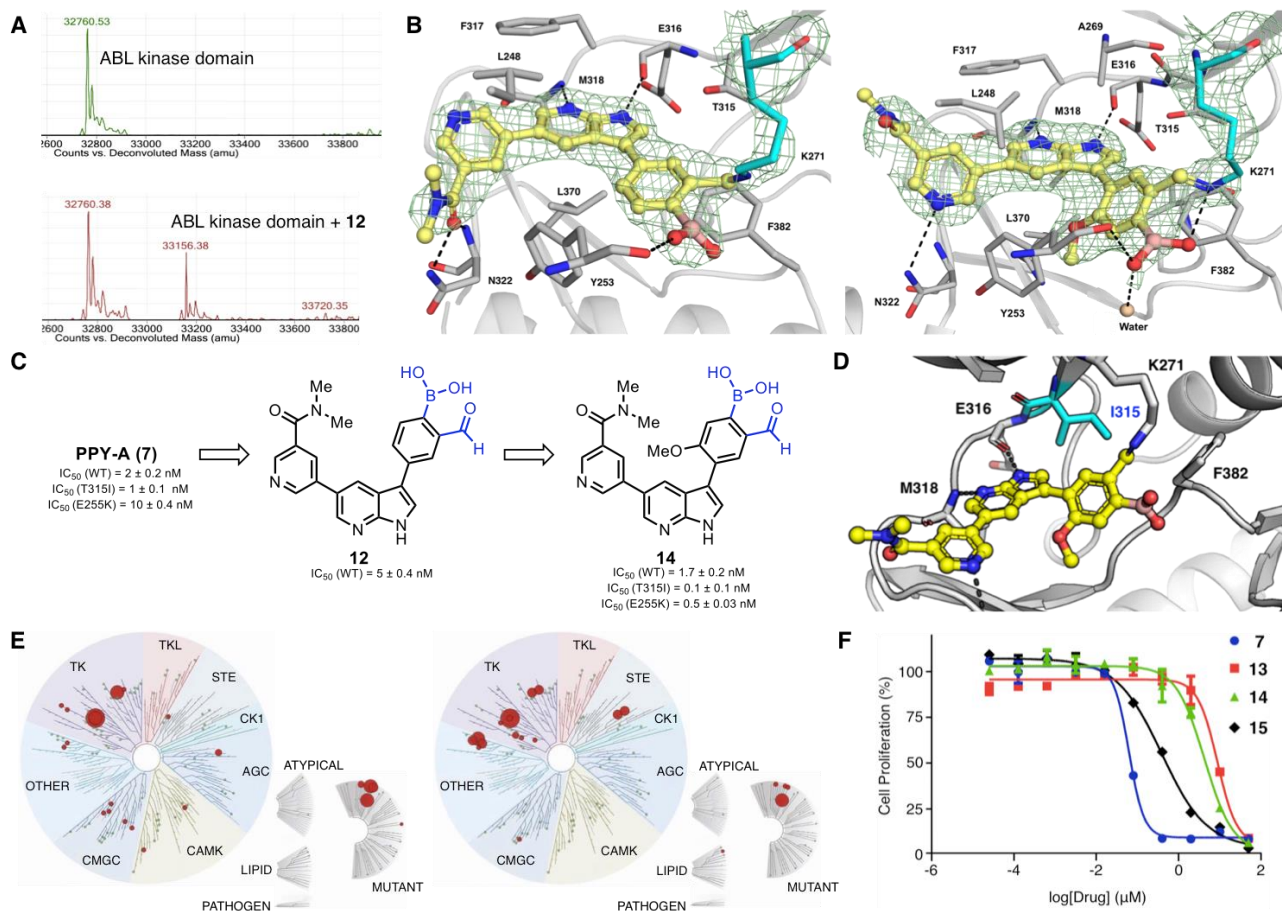


**Figure 2.** (A) Mass spectrometric analysis of the ABL kinase domain-12 complex. (B) Cocrystal structures of the ABL kinase domain with **12** (left) and **14** (right) showing the composite omit map (2F<sub>o</sub>-F<sub>c</sub>) contoured to 1σ in green mesh. The front loop was removed for better visibility. (C) Comparison of ABL inhibition (WT and mutants) of PPY-A (**7**), **12** and **14** after 6 or 12 h. (D) Modeled structure of ABL<sup>T315I</sup> kinase domain-**14** complex based on the obtained cocrystal structure of ABL<sup>WT</sup> kinase domain-**14** complex. (E) Dendrograms showing Kinome Scan™ of **7** (left) and **14** (right) at 1000 nM against 90 different kinases. (F) Anti-proliferative activity of **7**, **13**, **14** and **15** against K562 cells determined by CellTiter-Glo® viability assay.

(compound **9**). Introduction of a boronic acid functionality led to inhibitors **11** and **12**. As expected of covalent inhibitors, the enzyme inhibition of compound **12** improved from 83 nM ( $T = 0$  h) to 5 nM ( $T = 12$  h) as the incubation time was increased (Figure S3A). Compound **10** did not show time-dependence of the  $IC_{50}$ , suggesting that the presence of the boronic acid in **12** may have led to the formation of an iminoboronate.<sup>[33]</sup>

To determine whether **12** was selective towards the catalytic lysine in ABL, mass spectrometric analysis was performed. MALDI-TOF analysis suggested that a single lysine-modified covalent adduct was formed with an observed  $m/z$  of 33156.38 Da (Figure 2A; compared to calculated mass of 33156.59 Da). The reaction did not reach completion regardless of the concentration (up to 1 mM) and incubation time (up to 24 h) of **12**, indicating that an equilibrium was established.<sup>[30,31]</sup> Since the OMe group in **7** was important for ABL inhibition, the same functionality was added to **12**, providing compound **14** which was synthesized via a similar route (Scheme 1, Figure S6C). As expected, **14** showed time-dependent  $IC_{50}$  values against ABL from 13 nM at 0 h to 1.7 nM after 12 h (Figure 2C); further testing of **7** and **14** against two ABL mutants indicated that **14** was about ten-fold more potent against both ABL<sup>T315I</sup> and ABL<sup>E255K</sup> than **7**, and at the same time also showed time-dependent inhibition against both mutants (Figures S3C and S3D). In particular, **14** demonstrated an improved potency from 25 nM ( $T = 0$  h) to 0.1 nM ( $T = 6$  h) against ABL<sup>T315I</sup> (250-fold improvement) and from 43 nM ( $T = 0$  h) to 0.5 nM ( $T = 12$  h) against ABL<sup>E255K</sup> (100-fold improvement). The effect of point mutation on restricting access to the binding pocket or stabilizing certain protein conformations has been shown to adversely affect drug binding which tends to favor only a very specific target conformation;<sup>[10]</sup> however, our examples showed that targeting the catalytic lysine residues gave an advantage in this context.

The X-ray cocrystal structures of **12** and **14** with the ABL kinase domain (229-510) were solved up to 2.7 Å and 2.3 Å resolution, respectively, giving more insights into how this particular warhead interacts with the catalytic lysine residue (Figure 2B; PDB IDs: 7CC2 and 7DT2); the continuous electron density from K271 in the ABL kinase domain to **12** and **14** suggests that the imine product was formed. We did not however observe the formation of the expected dative bond between the imine nitrogen and the boron atom. In fact, the lone pair of the imine appeared to be orientated away from the boron atom in both crystal structures. One of the reasons could be due to the vast structural difference between the macromolecule-inhibitor complex and small molecules given the tight binding pocket of a protein target (our data <sup>11</sup>B NMR showed that an iminoboronate could be captured for small molecules, Figure S14). Since the biochemical assays and the MALDI-TOF analysis suggested that the boronic acid plays an important role in the formation of the adduct,

we propose that the obtained cocrystal structures had successfully captured the key intermediate during the formation of the iminoboronates. Given the fact that **14** was able to potently inhibit ABL<sup>T315I</sup> while imatinib and second-generation kinase inhibitors such as nilotinib, dasatinib failed to do so,<sup>[32]</sup> we next rationalized this observation by using the newly obtained structural data (Figure 2D); by building a modeled structural complex of **14** and ABL kinase domain in which the T315 residue was artificially changed to I315, we observed no steric clash upon inhibitor binding. Imatinib, nilotinib and dasatinib possess crucial elongated structures that are extended to the back cleft of the ATP binding pocket in ABL, and T315I point mutation was expected to restrict access to the hydrophobic region at the rear of this pocket.<sup>[32]</sup> This is not the case for **14** which does not have any substituent that occupies this pocket. Finally, **14** demonstrated better biochemical activity than that of **7** due to apparent covalent modification,<sup>[34]</sup> and the incorporation of both boronic acid and aldehyde did not appear to cause any steric clash with the I315 residue.

The kinetic parameters of inactivation were next determined to better understand the non-bonded interaction of **12** and **14** with the kinase (Figures S4);<sup>[34]</sup> both compounds showed similar  $k_{inact}$  values. while **14** had a smaller  $K_i$  compared to that of **12**, thus confirming that the critical role of OMe in **14** for increased affinity between the inhibitor and the ABL kinase domain.

One of the potential concerns for covalent inhibitors like **14**, which target a key amino acid in the active site of kinases, is the selectivity. We therefore carried out Kinome Scan<sup>TM</sup> with a panel of ~100 protein kinases (Figure 2E); results showed highly similar interaction maps for compounds **7** (left) and **14** (right), suggesting that the degree of compound selectivity largely depended on the initial step of molecular recognition presumably due to the moderately reactive 2-carbonyl boronic acid warhead in **14**. The conclusion was further strengthened by the selectivity scores (Table S4). To evaluate the anti-proliferative activity of this class of inhibitors, compounds **7** and **14**, as well as reference compounds **13** and **15** (boronic acid-free versions of **14**; see Figure 1D), were tested in K562 cells. As shown in Figure 2F, compound **7** showed  $GI_{50}$  of 0.114  $\mu$ M whereas compounds **13**, **14** and **15** were less active with  $GI_{50}$  values of 3.85  $\mu$ M, 1.19  $\mu$ M and 0.384  $\mu$ M, respectively. In an attempt to understand the loss of activity, the cell permeability of three compounds were tested (Tables S5 and S6); Compound **13** showed poor recovery rates which could be due to metabolism of the aldehyde functional group.<sup>[35]</sup> The 10-fold improvement in the anti-proliferative activity of its ketone counterpart (e.g. **15**;  $GI_{50} = 0.384 \mu$ M) suggests that the aldehyde might not be the optimal choice for this scaffold in the cellular systems.

Finally, to evaluate the proteome-wide reactivity and potential off-targets of **14** in live mammalian cells, we synthesized its alkyne-containing analog (**16**; Scheme

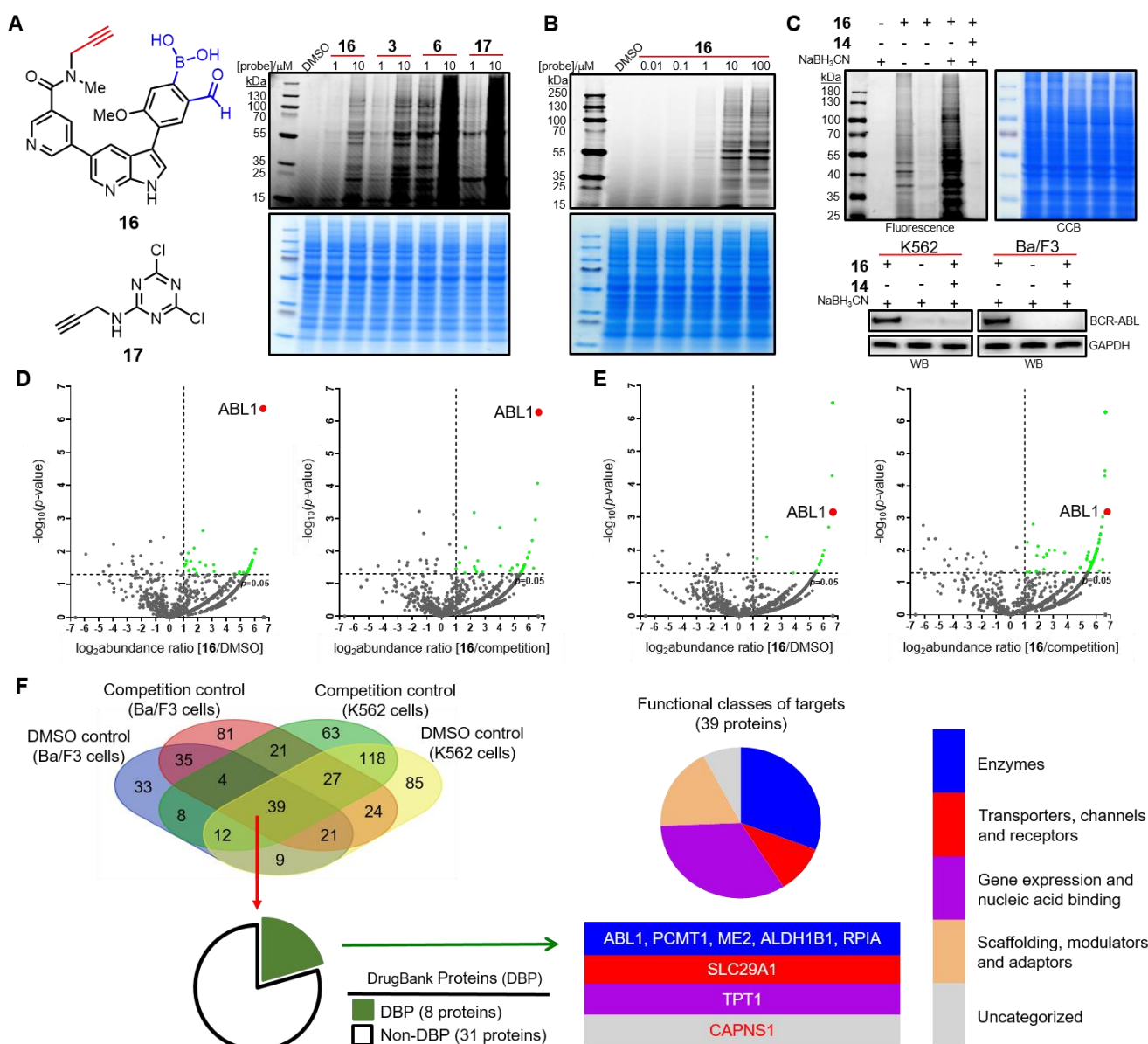


**Figure 3.** (A) Proteome reactivity profiles of compound **16** compared to **3**, **6** and **17** in K562 cell lysates (in PBS with 0.1% Triton, pH 7.5). (Top): in-gel fluorescence scanning; (Bottom): Coomassie staining (CBB). (B) Concentration-dependent proteomic reactivity profiles of **16** (0–100  $\mu$ M) in Ba/F3 cells overexpressing BCR-ABL<sup>WT</sup>. (C) Effect of washing by cold acetone and cold methanol of probe-labeled K562 (see Figure S13 for corresponding Ba/F3 results) lysates in the absence and presence of excess NaBH<sub>3</sub>CN (top); Western blotting (WB) detection of BCR-ABL<sup>WT</sup> in lysates of both K562 and Ba/F3 cells following pull-down (PD) assays. GAPDH = loading control. (D/E) Volcano plots of potential cellular targets of **16** from probe-treated K562 and Ba/F3 cell lysates, respectively. (F) Data analysis of shared targets identified from chemoproteomic experiments in (D/E). See Figures S12, S13 and Table S7 for details.

1) and carried out large-scale chemoproteomic studies (Figure 3).<sup>[36]</sup> We first compared the proteome reactivity of the aldehyde-boronic acid moiety to other well-known lysine-targeting functionalities by using lysates from K562 cells (Figure 3A);<sup>[17,18]</sup> in-gel fluorescence scanning analysis of probe-labeled lysates, followed by CuAAC with rhodamine azide,<sup>[37]</sup> showed that **3** demonstrated better selectivity at both 1  $\mu$ M and 10  $\mu$ M when compared to **6** and **17** which are known lysine-reactive electrophiles, but was predictably less selective compared to the kinase-targeting **16**, suggesting that molecular recognition was the dominant factor for similar compounds that contain low-reactivity

electrophiles such as iminoboronates.<sup>[38,39]</sup> In **16**-treated samples, we observed a concentration-dependent labeling of proteomes, with saturated fluorescence signals at  $\sim$ 10  $\mu$ M of the probe (Figure 3B). We next repeated the labeling experiment in the presence of NaBH<sub>3</sub>CN which helped trap the reversible covalent iminoboronates into more stable amine adducts (Figure 3C); a concomitant increase in the fluorescence intensity of the **16**-labeled proteome was observed. In contrast, in the absence of NaBH<sub>3</sub>CN, washing the **16**-labeled proteome with cold acetone and methanol significantly reduced or abolished the labeling, thus confirming the reversibility of iminoboronate bond

(Figures S13 and S14). Upon further enrichment of the labeled proteomes by pull-down (PD) experiments followed by Western blotting (WB) analysis, we confirmed successful labeling of endogenous BCR-ABL from both K562 and Ba/F3 cell lysates (Figure 3C bottom). By using DMSO-treated and **14**-competed samples as controls, we carried out large-scale LC-MS analysis (Figures 3C-E, S11 and S12, Table S7).<sup>[22,36,37]</sup> Consistent with strong labeling shown by in-gel fluorescence scanning (Figure 3C), **16** captured a number of off-targets in addition to the expected BCR-ABL (highlighted in red in Figure 3D/E). Upon combining analyses of enriched hits from **16**-labeled proteomes of both K562 and Ba/F3 cells, we identified a total of 39 potential cellular targets out of which 8 were DrugBank proteins including ABL1, PCMT1, ME2, ALDH1B1, RPIA, SLC29A1, TPT1 and CAPNS1 at a high confidence level (Figure 3F and Table S7). Unlike protein kinases which have a known catalytic lysine residue in their kinase active site, most of these shared targets possess solvent-exposed lysine residues, rendering them susceptible to probe labeling. Interestingly, ABL1 was the only kinase successfully identified from our experiments in both cell lines, indicating **16** was a selective ABL-targeting probe towards kinases.

## Conclusion

In summary, we have successfully demonstrated, for the first time, that the catalytic lysine of ABL can be selectively targeted by inhibitors bearing the aldehyde boronic acid moiety, leading to a reversible covalent adduct. The incorporation of the two substituents required for covalent bond formation reduced the affinity to the ABL active site; however, the slow formation of the iminoboronate led to highly potent inhibitors of ABL kinase and its mutants. We also showed that the aldehyde boronic acid, which is a low-reactivity electrophile, can be used to design highly selective kinase inhibitors by maximizing molecular recognition. Such compounds might be attractive tools for chemical biology studies given recent interests in the development of reversible covalent inhibitors,<sup>[29,31,40]</sup> but could also serve as potential drug candidates in cases where improved potency might be desirable once they are fully optimized.

## Acknowledgements

Financial support was provided by the Synthetic Biology Research & Development Programme (SBP) of National Research Foundation (SBP-P4 and SBP-P8) for Shao Q. Yao, the National Medical Research Council (NMRC) via the Open Fund – Young Individual Research Grant for Klement Foo and by the Agency for Science, Technology and Research (A\*STAR) via the A\*STAR Graduate Scholarship (AGS) for David Quach. Financial support from CAMS Innovation Fund for Medical Sciences (CIFMS) (2017-I2M-4-005) of China

is also acknowledged. The ABL protein construct and glycerol stock were prepared by Yvonne Y. W. Tan and Dario B. Heymann.

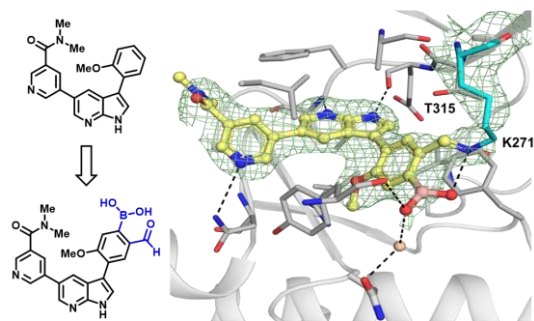
**Keywords:** cancer • lysine • covalent • reversible • proteomics

- [1] R. Kurzrock, J. U. Gutterman, M. Talpaz, *N. Engl. J. Med.* **1988**, *319*, 990–998.
- [2] T. G. Lugo, A. M. Pendergast, A. J. Muller, O. N. Witte, *Science* **1990**, *247*, 1079–1082.
- [3] E. Jabbour, H. Kantarjian, *Am. J. Hematol.* **2016**, *91*, 252–265.
- [4] H. M. Kantarjian, M. Baccarani, E. Jabbour, G. Saglio, J. E. Cortes, *Clin. Cancer Res.* **2011**, *17*, 1674–1683.
- [5] Z. Iqbal, A. Aleem, M. Iqbal, M. I. Naqvi, A. Gill, A. S. Taj, A. Qayyum, N. ur-Rehman, A. M. Khalid, I. H. Shah, M. Khalid, R. Haq, M. Khan, S. M. Baig, A. Jamil, M. N. Abbas, M. Absar, A. Mahmood, M. Rasool, T. Akhtar, *PLoS One* **2013**, *8*, e55717.
- [6] T. Anagnostou, M. R. Litzow, *Blood Lymphat. Cancer* **2017**, *2018*, 1–9.
- [7] D. S. Johnson, E. Weerapana, B. F. Cravatt, *Future Med. Chem.* **2010**, *2*, 949–964.
- [8] A. Chaikuad, P. Koch, S. A. Laufer, S. Knapp, *Angew. Chem. Int. Ed.* **2018**, *57*, 4372–4385.
- [9] Z. Zhao, P. E. Bourne, *Drug Discov. Today* **2018**, *23*, 727–735.
- [10] J. Engel, J. Lategahn, D. Rauh, *ACS Med. Chem. Lett.* **2016**, *7*, 2–5.
- [11] S-H. I. Ou, *Crit. Rev. Oncol. Hematol.* **2012**, *83*, 407–421.
- [12] Q. S. Liu, Y. Sabnis, Z. Zhao, T. H. Zhang, S. J. Buhrlage, L. H. Jones, N. S. Gray, *Chem. Biol.* **2013**, *20*, 146–159.
- [13] S. Niessen, M. M. Dix, S. Barbas, Z. E. Potter, S. Lu, O. Brodsky, S. Planken, D. Behenna, C. Almaden, K. S. Gajiwala, K. Ryan, R. Ferre, M. R. Lazear, M. M. Hayward, J. C. Kath, B. F. Cravatt, *Cell Chem. Bio.* **2017**, *24*, 1388–1400.
- [14] F. Rossari, F. Minutolo, E. Orciuolo, *J. Hematol. Oncol.* **2018**, *11*, 1–14.
- [15] A. C. Carrera, K. Alexandrov, T. M. Roberts, *Proc. Natl. Acad. Sci. U. S. A.* **1993**, *90*, 442–446.
- [16] R. Liu, Z. Yue, C. C. Tsai, J. Shen, *J. Am. Chem. Soc.* **2019**, *141*, 6553–6560.
- [17] D. A. Shannon, R. Banerjee, E. R. Webster, D. W. Bak, C. Wang, E. Weerapana, *J. Am. Chem. Soc.* **2014**, *136*, 3330–3333.
- [18] C. C. Ward, J. L. Kleinman, D. K. Nomura, *ACS Chem. Biol.* **2017**, *12*, 1478–1483.
- [19] A. Cuesta, J. Taunton, *Annu. Rev. Biochem.* **2019**, *88*, 365–381.
- [20] M. Gehringer, S. A. Laufer, *J. Med. Chem.* **2019**, *62*, 5673–5724.
- [21] S. M. Hacker, K. M. Backus, M. R. Lazear, S. Forli, B. E. Correia, B. F. Cravatt, *Nat. Chem.* **2017**, *9*, 1181–1190.
- [22] Q. Zhao, X. Ouyang, X. Wan, K. S. Gajiwala, J. C. Kath, L. H. Jones, A. L. Burlingame, J. Taunton, *J. Am. Chem. Soc.* **2017**, *139*, 680–685.
- [23] S. E. Dalton, L. Dittus, D. A. Thomas, M. A. Convery, J. Nunes, J. T. Bush, J. P. Evans, T. Werner, M. Bantscheff, J. A. Murphy, S. Campos, *J. Chem. Am. Soc.* **2018**, *140*, 932–939.
- [24] U. P. Dahal, A. M. Gilbert, R. S. Obach, M. E. Flanagan, J. M. Chen, C. Garcia-Irizarry, J. T. Starr, B. Schuff, D. P. Uccello, J. A. Young, *Med. Chem. Commun.* **2016**, *7*, 864–872.
- [25] J. Pettinger, K. Jones, M. D. Cheeseman, *Angew. Chem. Int. Ed.* **2017**, *56*, 15200–15209.
- [26] P. Martín-Gago, C. A. Olsen, *Angew. Chem. Int. Ed.* **2019**, *58*, 957–966.
- [27] L. H. Jones, *Angew. Chem. Int. Ed.* **2018**, *57*, 9220–9223.
- [28] D. E. Mortenson, G. J. Brightly, L. Plate, G. Bare, W. Chen, S. Li, H. Wang, B. F. Cravatt, S. Forli, E. T. Powers, K. B. Sharpless, I. A. Wilson, J. W. Kelly, *J. Am. Chem. Soc.* **2018**, *140*, 200–210.
- [29] I. M. Serafimova, M. A. Pufall, S. Krishnan, K. Duda, M. S. Cohen, R. L. Maglathlin, J. M. McFarland, R. M. Miller, M. Frödin, J. Taunton, *Nat. Chem. Biol.* **2012**, *8*, 471–476.

- 
- [30] S. Cambray, J. Gao, *Acc. Chem. Res.* **2018**, *51*, 2198-2206.
- [31] G. Akçay, M. A. Belmonte, B. Aquila, C. Chuaqui, A.W. Hird, M. L. Lamb, P. B. Rawlins, N. Su, S. Tentarelli, N. P. Grimster, Q. Su, *Nat. Chem. Biol.* **2016**, *12*, 931-936.
- [32] T. Zhou, L. Parillon, F. Li, Y. Wang, J. Keats, S. Lamore, Q. Xu, W. Shakespeare, D. Dalgarno, X. Zhu, *Chem. Biol. Drug Des.* **2007**, *70*, 171-181.
- [33] P. M. S. D. Cal, J. B. Vicente, E. Pires, A. V. Coelho, L. F. Veiros, C. Cordeiro, P. M. P. Gois, *J. Am. Chem. Soc.* **2012**, *134*, 10299-10305.
- [34] R. A. Bauer, *Drug Discov. Today* **2015**, *20*, 1061-1073.
- [35] L. A. Admed, H. Younus, *Drug Metab. Rev.* **2019**, *51*, 42-64.
- [36] B. R. Lanning, L. R. Whitby, M. M. Dix, J. Douhan, A. M. Gilbert, E. C. Hett, T. O. Johnson, C. Joslyn, J. C. Kath, S. Niessen, L. R. Roberts, M. E. Schnute, C. Wang, J. J. Hulce, B. Wei, L. O. Whiteley, M. M. Hayward, B. F. Cravatt, *Nat. Chem. Biol.* **2014**, *10*, 760-767.
- [37] H. Shi, C.-J. Zhang, G. Y. J. Chen, S. Q. Yao, *J. Am. Chem. Soc.* **2012**, *134*, 3001-3014.
- [38] K. M. Backus, B. E. Correia, K. M. Lum, S. Forli, B. D. Horning, G. E. González-Páez, S. Chatterjee, B. R. Lanning, J. R. Teijaro, A. J. Oison, D. W. Wolan, B. F. Cravatt, *Nature* **2016**, *534*, 570-574.
- [39] S. Pan, S. Y. Jang, S. S. Liew, J. Fu, D. Wang, J. S. Lee, S. Q. Yao, *Angew. Chem. Int. Ed.* **2018**, *57*, 579-583.
- [40] a) W.-H. Guo, X. Qi, X. Yu, Y. Liu, C.-I. Chung, F. Bai, X. Lin, D. Lu, L. Wang, J. Chen, L. H. Su, K. J. Nornie, F. Li, M. C. Wang, X. Shu, J. N. Onuchic, J. A. Woyach, M. L. Wang, J. Wang, *Nat. Commun.* **2020**, *11*, 4268; b) R. Gabizon, A. Shraga, P. Gehrtz, E. Livnah, Y. Shorer, N. Gurwicz, L. Avram, T. Unger, H. Aharoni, S. Albeck, A. Brandis, Z. Shulman, B.-Z. Katz, Y. Herishanu, N. London, *J. Am. Chem. Soc.* **2020**, *142*, 11734-11742.

---

## Entry for the Table of Contents



- ✓ Reversible covalent BCR-ABL inhibitor
- ✓ Improved potency against ABL<sup>T315I</sup>
- ✓ Targeting kinome-conserved lysine
- ✓ Activity-based protein profiling

Using the iminoboronate chemistry, we report the first successful examples of catalytic lysine-targeting reversible covalent BCR-ABL inhibitors which inhibited both ABL<sup>WT</sup> and ABL<sup>T315I</sup> at improved nanomolar potency. We also demonstrated for the first time how the study of off-targets for this class of compounds could be performed using activity-based protein profiling and proteomic mass spectrometry.